SUBJECT: **The level of the photometer background signal from the optics**

PREPARED BY: **Tony Richards**

KEYWORDS: **background, thermal, photometer**

COMMENTS: **Direct radiative signals from the FIRST telescope and BOL photometer have been estimated and found to nearly equal or exceed, depending on the waveband, the figures for the maximum signal, in watts, desired on the BOL detectors.**
optics

DISTRIBUTION

A. Richards	(RAL)	•
M Caldwell	(RAL)	•
B.Swinyard	(RAL)	•
M.Griffin	(QMW)	•
E.Atad	(ROE)	•
Project Office	(RAL)	•

CONTENTS

FIGURES

TABLES

1.0 Introduction

The proposed design for the BOL photometer optics is illustrated in figure 1. It shows the six (possibly seven) optical surfaces, labelled M2 to M8 (the FIRST telescope mirrors being M1 and M2), which are needed after the telescope focal plane in order to transfer the energy in the BOL FOV to the detector arrays. This note summarises a first attempt at estimating the level of background signals which reach the detectors as a result of

1. Direct radiation from the optical components
2. Diffracted radiation originating from out-of-FOV telescope surfaces

The data used as a basis for the calculations are set out below and the author welcomes feedback on the accuracy or otherwise of the numbers, so that the background estimates can be corrected and updated in response to any changes that might be made or justified in the light of the evolution of the FIRST-BOL design.

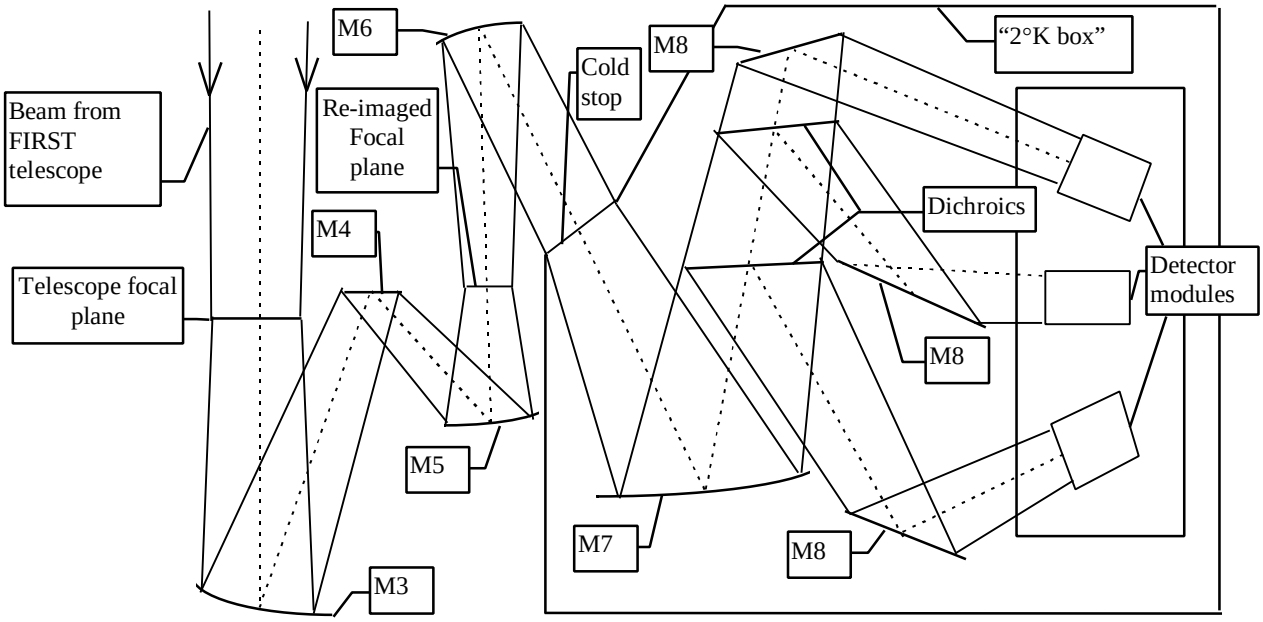

Figure 1 Proposed BOL optical layout

2.0 Assumptions and formulae

2.1 Formula for the power radiated from each component into the instrument FOV

The expression used for the total wavelength integrated power P(ε,T,Ac,Ωc) in watts radiated by a component with emissivity **e** at temperature **T** towards a detector is (with **s** = Stefan's constant = 5.67*10^-8 watt/metre^2/deg^4)

$$P(e,T,Ac,Wc) = e\frac{s*T^4}{p}*Ac*Wc \qquad (1)$$

Ac is the area in square metres of the component 'seen' by a 'detector' which appears to occupy a fov covering Ωc steradians, viewed from the component. The product Ac*Ωc = A*Ω is the throughput which is constant at all points in an optical system (if we ignore diffraction), up to the last aperture stop before the final image plane at the detector. The power integrated over the BOL waveband, P(ε,T,λmin,λmax,Ac,Ωc) was found from the following expression,

$$P(e,T,\ l\,min,\ l\,max,Ac,Wc) = P(e,T,Ac,Wc) * F(T,\ l\,min,\ l\,max) = \frac{e * Ac * Wc * s\ * T^4}{p} * F(T,\ l\,min,\ l\,max) \qquad (2)$$

F(T, λmin,λmax) is the fraction of the total black-body spectral power emitted within the specified waveband:

$$F(T,\ l\,min,\ l\,max) = \left(\int_{l\,min}^{l\,max} \frac{2phc^2\ l^{-5}}{exp(hc/\ lkT) - 1} d\,l \right) / \left(s\ * T^4 \right) \qquad (3)$$

MATHCAD was used to evaluate the integral in eq(3) as a summation at 1/4 micron intervals multiplied by 1/4 micron. Table 5 gives F(T, λmin,λmax) and P(ε,T,λmin,λmax,Ac,Ωc) for each component.

2.2 Optics AW - value (throughput)

For the FIRST telescope and the BOL optics, we have taken an AΩ - value commensurate with an effective **3.2 metre** diameter primary mirror imaging a **5.2 arc minute** diameter FOV (radial FOV size = 2.6 arc minute = 0.04333 degree). This gives

$$A.W = \left(\frac{p\ * 3.2^2}{4} \right) * \left((p\ /\ 4) * \left(\frac{5.6 * p}{60 * 180} \right)^2 \right) = 1.445 * 10^{-5}\ metre^2 - steradian \qquad (4)$$

This figure can be appropriately scaled to any diameter telescope DTEL (in metres) and FOV diameter DFOV (in arc minutes) by multiplying by $(DTEL/3.2)^2 * (DFOV/5.6)^2$

2.3 Component Emissivities

The broadband emissivities of all mirrors have been set to **e=0.01,** effectively assuming very high 99 % (100*(1-ε)) reflectivity coatings for all optical surfaces. Results can be easily scaled to emissivities higher than this likely minimum.

2.4 Optical Component Temperatures

The temperatures assumed for the telescope components (M1 and M2) were T=80°K. The temperatures assumed for the other 6 surfaces (M3 to M8) were T=15°K for M3-M5, T=4°K for M6 and T=2°K for M7 and M8. These were felt to be reasonable guesstimates proposed by those present at the June meeting of the FIRST-BOL consortium members.

2.5 The Total waveband covered by BOL

The complete waveband which BOL is deemed to cover was taken to be λmin = 200μ, λmax= 650μ.

2.6 The separate wavebands covered by the three BOL detector arrays

The complete waveband which BOL is intended to cover will be divided into three separate wavebands, nominally assumed to be as given in table 1 below. Each waveband will have its own detector array. Wavelength separation will be achieved using dichroic filters in the 2°K box.

Table 1. BOL wavebands

waveband	λmin, microns	λmax, microns
1	200	300
2	300	400
3	400	650

2.7 The Detector sizes in each waveband

The BOL FOV will be covered by a different number of detectors in each waveband. Table 2 shows estimates of the number of detectors which can usefully be employed in each waveband (taken from a note by M.Griffin and B.Maffei, 21/3/97). It is assumed that the physical detector sizes (pixels) will be different in each waveband to ensure that the same total FOV size is covered in each and so that a single AΩ value can be used for all three wavebands.

Table 2. Number of pixels/detectors in each BOL waveband

waveband	λmin (microns)	λmax (microns)	number of pixels
1	200	300	61
2	300	400	37
3	400	650	19

2.8 Overall filter transmission

In order to allow for the effect of the filters, the following transmission factors have been used for each waveband:

Table 3. Filter transmission factors

waveband	λmin (microns)	λmax (microns)	Transmission factor
1	200	300	0.3
2	300	400	0.3
3	400	650	0.3

3.0 Integrated power radiated by optics towards the BOL detectors

The most recent design for BOL involves eight optical surfaces (including the two telescope mirrors but without counting any filters required - see figure 1). The table below shows estimates of the the radiant power from each component (separately integrated over all wavelengths, eq(1), and integrated over the BOL waveband of 200-650 microns, eq(3)) which is emitted directly into a solid angle covering the whole FOV covered by all the detectors. All quantities given or used in the table have been defined and/or justified above.

Table 4. Integrated power from each component radiated towards the BOL FOV

Component	T°K	ε	P(ε,T,Ac,Ωc) watts	F(T, 200μ,650μ)	P(ε,T,λmin,λmax,Ac,Ωc) watts
Primary(M1)	80	0.01	1.07*10^-7	0.025432	0.0272*10^-7
Secondary(M2)	80	0.01	1.07*10^-7	0.025432	0.0272*10^-7
M3	15	0.01	1.32*10^-10	0.636075	0.8396*10^-10
M4	15	0.01	1.32*10^-10	0.636075	0.8396*10^-10
M5	15	0.01	1.32*10^-10	0.636075	0.8396*10^-10
M6	4	0.01	6.67*10^-13	0.183191	1.2219*10^-13
M7	2	0.01	4.17*10^-14	0.004343	0.0181*10^-14 see note
M8	2	0.01	4.17*10^-14	0.004343	0.0181*10^-14 see note

NOTE. Whereas it is proposed that the band-limiting of power from M1-M6 be imposed using a filter at the image of the aperture stop between M6 and M7 (which is the proposed location of the aperture in the '2°K box' which is intended to surround the optics subsequent to M6), the band-limiting of power from M7 and M8 will not be possible, because there must be at least one component at 2°K which the detector array sees unfiltered, unless the detector array is isolated at a lower temperature and an additional band-limiting filter at this lower temperature can be located in front of it.

Table 5. Integrated power from each component radiated towards each detector in each waveband

Component	T °K	ε	P(ε,T,Ac,Ωc) watts unfiltered power whole FOV	F(T, 200,300) band 1	F(T, 300,400) band 2	F(T, 400,650) band 3	Filtered Power,watts per pixel, band 1	Filtered Power,watts per pixel, band 2	Filtered Power,watts per pixel, band 3	Reflectivity factor (1-ε)^(8-n) for mirror Mn,n=1,2...8	Filter Transmission factor
M1	80	0.01	1.07*10^-7	0.017517	0.004859	0.002952	3.0727*10^-11	1.4052*10^-11	1.6624*10^-11	0.9321	0.3
M2	80	0.01	1.07*10^-7	0.017517	0.004859	0.002952	3.0727*10^-11	1.4052*10^-11	1.6624*10^-11	0.9415	0.3
M3	15	0.01	1.32*10^-10	0.291783	0.173938	0.171244	0.6314*10^-12	0.6205*10^-12	1.1897*10^-12	0.951	0.3
M4	15	0.01	1.32*10^-10	0.291783	0.173938	0.171244	0.6314*10^-12	0.6205*10^-12	1.1897*10^-12	0.9606	0.3
M5	15	0.01	1.32*10^-10	0.291783	0.173938	0.171244	0.6314*10^-12	0.6205*10^-12	1.1897*10^-12	0.9703	0.3
M6	4	0.01	6.67*10^-13	0.002125	0.017268	0.163532	2.3236*10^-17	3.1129*10^-16	5.7408*10^-15	0.9801	0.3
M7	2	0.01	4.17*10^-14	9.367*10^-8	1.641*10^-5	0.004306	6.4033*10^-23	1.8495*10^-20	0.9451*10^-17	0.99	0.3
M8	2	0.01	4.17*10^-14	9.367*10^-8	1.641*10^-5	0.004306	6.4033*10^-23	1.8495*10^-20	0.9451*10^-17	1.	0.3
ALL				TOTAL WATTS EACH PIXEL→			17.817*10^-12	8.435*10^-12	10.374*10^-12		

Table 6. Fractions of integrated power from each component, in each waveband

Component	T°K	ε	Fraction of Filtered Power per pixel, band 1	Fraction of Filtered Power per pixel, band 2	Fraction of Filtered Power per pixel, band 3
M1	80	0.01	0.48225	0.46584	0.4481
M2	80	0.01	0.48711	0.47054	0.45262
M3	15	0.01	0.01011	0.02099	0.03272
M4	15	0.01	0.01021	0.0212	0.03305
M5	15	0.01	0.01032	0.02141	0.03338
M6	4	0.01	0.0	0.0	0.0
M7	2	0.01	0.0	0.0	0.0
M8	2	0.01	0.0	0.0	0.0

Table 5. Integrated power from each component radiated towards each detector in ea

Component	T °K	ε	P(ε,T,Ac,Ωc) watts unfiltered power whole FOV	F(T, 200,300) band 1	F(T, 300,400) band 2	F(T, 400,650) band 3	Filtered Power,watts per pixel, band 1	Filtered Power,watt per pixel, ba 2
M1	80	0.01	1.07*10^-7	0.017517	0.004859	0.002952	3.0727*10^-11	1.4052*10^-
M2	80	0.01	1.07*10^-7	0.017517	0.004859	0.002952	3.0727*10^-11	1.4052*10^-
M3	15	0.01	1.32*10^-10	0.291783	0.173938	0.171244	0.6314*10^-12	0.6205*10^-
M4	15	0.01	1.32*10^-10	0.291783	0.173938	0.171244	0.6314*10^-12	0.6205*10^-
M5	15	0.01	1.32*10^-10	0.291783	0.173938	0.171244	0.6314*10^-12	0.6205*10^-
M6	4	0.01	6.67*10^-13	0.002125	0.017268	0.163532	2.3236*10^-17	3.1129*10^-
M7	2	0.01	4.17*10^-14	9.367*10^-8	1.641*10^-5	0.004306	6.4033*10^-23	1.8495*10^-
M8	2	0.01	4.17*10^-14	9.367*10^-8	1.641*10^-5	0.004306	6.4033*10^-23	1.8495*10^-
ALL				TOTAL WATTS EACH PIXEL→			17.817*10^-12	8.435*10^-

Table 6. Fractions of integrated power from each component, in each waveb

Component	T°K	ε	Fraction of Filtered Power per pixel, band 1	Fraction of Filtered Power per pixel, band 2	Fraction of Filtered Power per pixel, band 3
M1	80	0.01	0.48225	0.46584	0.4481
M2	80	0.01	0.48711	0.47054	0.45262
M3	15	0.01	0.01011	0.02099	0.03272
M4	15	0.01	0.01021	0.0212	0.03305
M5	15	0.01	0.01032	0.02141	0.03338
M6	4	0.01	0.0	0.0	0.0
M7	2	0.01	0.0	0.0	0.0
M8	2	0.01	0.0	0.0	0.0

4.0 Power radiated towards each pixel in each of 3 wavebands in the BOL FOV

Given that the BOL waveband is divided into three, table 5 above shows the result of extending the computations summarised in table 4 to take into account this division and the fact that the FOV will be divided between a number of detectors/pixels. Table 5 shows the results of

1. Introducing the fractional power covering each waveband and
2. dividing that power by the number of detectors

in order to obtain a contribution expected to the background at each detector in each band from each component. Finally, the summed total, of contributions from all optical components weighted by the reflectivities (1-ε) of each component which follows it in the optical train and by the overall filter transmission factors in table 3, are given for each waveband

5.0 Permitted maximum background power levels

A maximum allowed background power in a detector pixel has been stated. These values are given in column 4, table 7, along with the estimated total direct radiated power per pixel in each band (column 5), to permit easy comparison.

Table 7. Maximum permitted background power/pixel compared with estimates (table 5)

waveband	λmin, microns	λmax, microns	Max. Permitted Power WATTS	Estimated direct background from all mirrors, WATTS
1	200	300	22.0*10^-12	17.817*10^-12
2	300	400	10.0*10^-12	8.435*10^-12
3	400	650	4.0*10^-12	10.374*10^-12

6.0 Comparison of direct radiated background and permitted maximum background

The final row in table 5 indicates the sort of background power levels to expect in a pixel in each waveband, for the conditions (temperatures, emissivities, throughput etc.) described above. They are repeated in table 7 along with the suggested maximum permitted values.

The totals for direct radiation received per pixel in each waveband are, as expected, dominated by the contributions from the primary and secondary telescope mirrors. With the present conditions assumed for the telescope (ε=0.01, T=80K), table 7 shows that the band 3 background already exceeds the budgeted maximum permitted power by a factor 2.5. In bands 1 and 2, the background values are only about 20 percent below the budgeted maxima for the bands, leaving little or no margin for telescope emissivities to increase above ε=0.01.

Table 6 shows that the fractions of the total background signal contributed directly by the three mirrors (M3, M4, M5) taken to be at 15°K are roughly 3%, 6% and 10% of the total contributions in bands 1, 2 and 3 respectively. Thus, moderate changes in emissivity values for these mirrors will have marginal effects on the totals for each waveband. The fractions of the total background signal contributed directly by the three mirrors (M6, M7, M8) taken to be at 4°K or below are negligible when compared to the contributions made by the other mirrors.

7.0 Possible Diffraction contributions

Given that the direct background contributions appear to be dominated by the two T=80K mirror surfaces, of major concern is the possibility that a further contribution from T>15K surfaces may occur due to radiation from the telescope tube and dewar walls between the secondary and the telescope focal plane above M3 being diffracted at M3 and other mirror surfaces/apertures which may be illuminated (see figure 2).

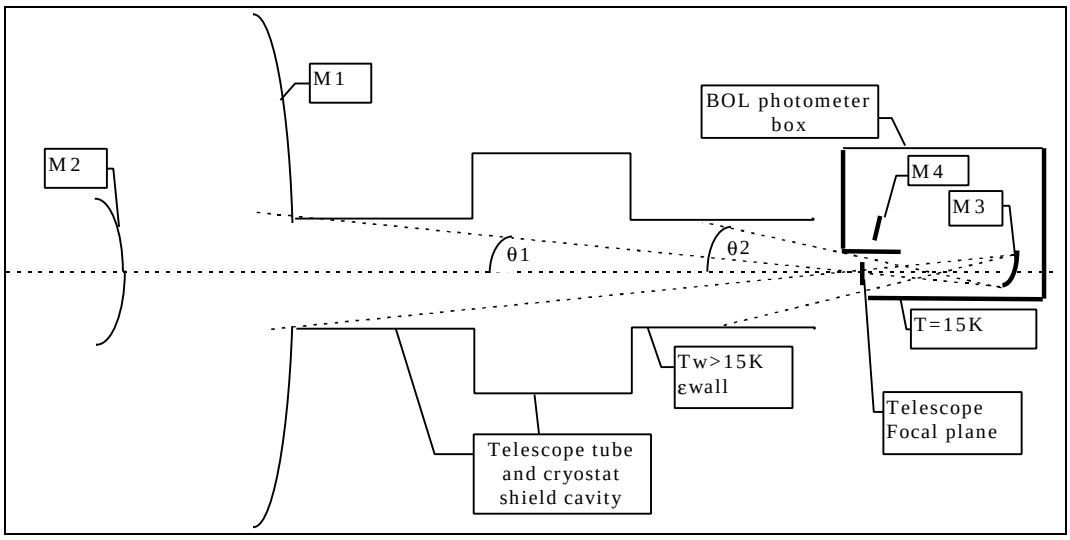

Figure 2 How T>15K radiation from higher emissivity surfaces can reach M3 and M4

Figure 2 shows the geometry in a schematic way. M3 (and M4, by reflection from M3) can receive radiation from the telescope and dewar walls over an angular range extending between angles θ1 and θ2 from a central axis through M3. Rough estimates for these boundary angles are given in table 8

Table 8 Estimated angular range for diffraction integration

Component→	M3
θ1	7 degrees
θ2	15 degrees

The model used to estimate the diffraction contribution is as follows. An area of a surrounding surface at angle Θ from the local reference direction radiates onto an aperture having diameter D. A fraction BDDF(Θ,λ)*Ωdet is scattered towards the detector, solid angle Ωdet. BDDF(Θ,λ) is some model for the Bi-directional Diffraction Distribution Function which expresses how radiation of wavelength λ is diffracted at the aperture through an angle Θ to send it towards the detector. The simplest function which can be used is eq(5) which approximates the Airy function for a circular aperture and which averages the effect of the high-frequency oscillations in the wings:

$$BDDF(Q) = \left(\frac{l}{D}\right) * \frac{1}{p^3 * sin(Q)^3} \qquad (5)$$

If εw = the emissivity of the Tw>15K surfaces (tube+cryostat walls) between the rear of the primary and the BOL entrance port, then a rough estimate of the diffraction contribution from a component can be expressed as an effective emissivity increment, δε(Tw,λ,D) at wavelength λ, for the illuminated aperture, diameter D, where

$$d\varepsilon(Tw,\ l, D) = ew(Tw) * \int_{q1}^{q2} 2p * BDDF(Q\ ,\ l).\cos(Q\ ).\sin(Q\ )dQ\ = ew(Tw) * (2p\,l\ / p^{3}D) * \left(\frac{1}{\sin(q1)} - \frac{1}{\sin(q2)}\right) \qquad (6)$$

εw and δε have been tagged with the temperature of the source of the emitted radiation, for the very good reason that, in order to compute the contribution to the radiative background power, this emissivity must be multiplied by the radiance of a blackbody at the same temperature Tw=80K as the source (telescope tube+cryostat walls) whose radiation illuminates the component, not the temperature of the component. Since the Tw=80K irradiance appears to dominate the direct background signal, a relatively small δε on a cold component due to radiation characterised by this warmer temperature can substantially increase the radiative background signal.

Equation (6) shows that there is a strong wavelength dependence, and since the BOL wavebands are quite wide, the emissivity increment will become a weighted integral δε(Tw,λbar,D), over the each BOL waveband, where

$$d\varepsilon(Tw,\ lbar, D) = \frac{\int_{l\,min}^{l\,max} \frac{(2phc^{2}\ l^{-5}) * d\varepsilon(Tw,\ l, D)}{\exp(hc\ /\ lkTw) - 1}\, d\,l}{\int_{l\,min}^{l\,max} \frac{2phc^{2}\ l^{-5}}{\exp(hc\ /\ lkTw) - 1}\, d\,l} = ew(Tw) * \left(\frac{2p\ *\ lbar(Tw)}{p^{3}D}\right) * \left(\frac{1}{\sin(q1)} - \frac{1}{\sin(q2)}\right) \qquad \textbf{(7)}$$

$$lbar(Tw) = \frac{\int_{l\,min}^{l\,max} \frac{(2phc^{2}\ l^{-5}) *\ l}{\exp(hc\ /\ lkTw) - 1}\, d\,l}{\int_{l\,min}^{l\,max} \frac{2phc^{2}\ l^{-5}}{\exp(hc\ /\ lkTw) - 1}\, d\,l} \qquad \textbf{(8)}$$

The weighted mean wavelength λbar(Tw) can be found for each waveband, given the temperature Tw. Table 9 gives the results of assuming Tw=80°K, 40°K and 15°K. The numbers are rounded to the nearest micron.

Table 9. Weighted mean wavelengths at Tw=80 °K, 40 °K and 15 °K for each BOL waveband

waveband	λmin, microns	λmax, microns	λbar(80K), microns	λbar(40K), microns	λbar(15K), microns
1	200	300	238	240	247
2	300	400	341	342	345
3	400	650	488	490	498

The final evaluation of the expression for δε(Tw,λbar,D), requires specifying an emissivity εw and a temperature Tw for the tube and cryostat internal walls and a diameter D for the mirror component M3.

7.1 Cryostat cavity internal wall temperature and emissivity

The FIRST phase 2 report emphasised the need to considerably reduce both the temperature and emissivity of the internal surfaces of the cryostat and telescope tube between the primary and the focal plane in order to get the radiated background onto the focal plane below acceptable levels. The report proposes that the emissivity should be reduced to εw=0.02 (a large reduction on the figure, εw=0.15, used in initial modelling), and that the ideal temperature for the baffle tube should be Tw=10K. The latter figure, when compared to the actual modelled temperature of Tw=97K for the internal cryostat/tube walls, appears optimistic. It was therefore decided not to use the (optimistic) figures of εw=0.02 and Tw=10K, but to use εw=0.15 and Tw=80K instead. These (possibly pessimistic) figures were felt to be more useful as the resulting estimates would give better indications of the magnitude of problems due to diffraction if they exist.

Table 10 Assumed cryostat/tube surface emissivity and temperature

cryostat/tube parameter	Value assumed
εw	0.15
Tw	80K

7.2 M3 diameter

The value for D, the diameter of M3, was taken to be the diameter of the beam footprint on M3 from a small region of the focal plane equal to that covered by a single detector pixel. This is justified on the basis that the view that a detector pixel has of M3 is restricted by at least one aperture stop between M3 and the detector. Therefore, the D is defined using the F/8 beam from the secondary and multiplying by the distance, 240 mm, between the focal plane and M3, giving

$$D = 240 / 8 = 30 mm \tag{9}$$

7.3 Estimated Emissivity increment due to diffraction

Having selected Tw=80K, the values for λbar evaluated at this temperature and given in table 9 can be used. With values now specified for all other parameters required, eq(7) can be reduced to the following equation

$$\delta\varepsilon(Tw = 80,\ lbar, D = 30) = 0.0044 * lbar \tag{10}$$

which is used to estimate the emissivity increments δε(Tw,λbar,D) for all three weighted mean wavelengths given in table 9 (λbar must be in mm, since eq(10) results from using D=30 mm in eq(7)). The results are given in table 11.

Table 11 Estimated emissivity increment for each waveband from T=80K surfaces

waveband	Tw	λbar(Tw), mm	δε(Tw,λbar,D)	δε(Tw,λbar,D)/0.01
1	80K	0.238	0.0010	0.1
2	80K	0.341	0.0015	0.15
3	80K	0.488	0.0021	0.21

7.4 Estimated diffraction contribution compared with direct signal

The emissivity increments shown in table 11 must be multiplied by the radiant signal from a T=80K black-body source and so the resulting contribution should be compared with the dominant contributors to the direct background signal at the same temperature, namely the primary and secondary telescope mirrors.

Relative to these sources, the diffraction contribution is in the ratio of the emissivity increment (ε=0.001 to 0.002) to the telescope mirror emissivity (ε=0.01). This ratio, for each waveband is given in table 11, column 5. Depending on the waveband, the estimated diffraction contribution appears to be between 10% and 20% of the direct contribution from one of the T=80K mirrors and hence between 5% and 10% of the direct contribution from both mirrors taken together. Looking at the figures in table 6, it thus appears that the diffraction contribution, from one mirror aperture illuminated by T=80K radiation, could exceed the direct contributions from all the BOL mirrors added together. However, it would still remain marginal compared to the direct signal from the telescope mirrors.

8.0 Summary and Conclusions

1. Direct radiative signals from the FIRST telescope and BOL optics have been estimated and been found to nearly equal or exceed, depending on the waveband, the figures for the maximum signal, in watts, desired

on the BOL detectors.

2. Changes to the telescope mirror emissivity will have a dramatic effect on the direct signal from them and hence on the feasibility of reaching the background limits presently proposed for the BOL photometer.

3. An estimate has been made for the contribution of diffracted out-of-FOV radiation originating from telescope tube and internal cryostat surfaces and it has been found to be marginal compared to the direct, in-FOV signal from the telescope mirrors.

4. Reduction of the emissivity of the internal cryostat/telescope tube surfaces from the presently-assumed figure of ε=0.15 will further reduce the significance of the diffraction contribution.